

LETTER TO THE EDITOR

Traits for chemical evolution in solar twins

Trends of neutron-capture elements with stellar age

Paula Jofré¹, Holly Jackson², and Marcelo Tucci Maia¹

¹ Núcleo de Astronomía, Universidad Diego Portales, Ejército 441, Santiago de Chile e-mail: paula.jofre@mail.udp.cl

² Department of Electrical Engineering and Computer Science, Massachusetts Institute of Technology, 50 Vassar Street, Cambridge, MA 02139, USA

Received November 20, 2019; accepted –

ABSTRACT

The physical processes driving chemical evolution in the Milky Way can be probed using the distribution of abundances in low-mass FGK type stars in space phase at different times. During their final stages of evolution stars experience nucleosynthesis several times, each at different timescales and producing different chemical elements, so finding abundance ratios that have simple variations across cosmic times remains a challenge. Using the sample of 80 solar twins for which ages and abundances of 30 elements were measured with high precision by [Bedell et al. \(2018\)](#), we searched for all possible abundance ratios combinations that show linear trends with age. We found 55 such ratios, all combining a n -capture element and another one produced by different nucleosynthesis channels. We recovered the ratios of $[Y/Mg]$, $[Ba/Mg]$ and $[Al/Y]$ reported previously in the literature, and found that $[C/Ba]$ had the largest dependency with age with a slope of 0.049 ± 0.003 dex/Gyr, imposing constraints on the magnitude of time dependency of abundance ratios in solar twins. Our results suggest using s -process elements, in lieu of Fe, as a reference for constraining chemical evolution models of the solar neighbourhood. Our study illustrates how a large variety of chemical elements measured from high resolution spectra is key in facing current challenges in understanding the formation and evolution of our Galaxy.

Key words. stars:abundances

1. Introduction

Chemical abundances of FGK low-mass stars have shown to be powerful tracers of the Milky Way evolution. This is because we assume the chemical composition of these stars' birthplaces is recorded in their photosphere. Since chemical composition evolves from one stellar generation to the next, when we combine this information with stellar age and phase-space, it is possible to reconstruct the different physical processes that shaped the Milky Way across cosmic times ([Freeman & Bland-Hawthorn 2002](#)).

The way chemistry in the Milky Way evolves is mainly due to stellar nucleosynthesis ([Nomoto et al. 2013](#); [Karakas & Lugaro 2016](#)). Newly synthesized metals are sent back to the interstellar medium and are recycled in new stars, and thereby their elemental abundances increase with time ([da Silva et al. 2012](#)). It is thus commonly assumed that the chemical composition of stars imprinted in their atmospheres remains unchanged in stellar lifetime, but it evolves in time through inheritance between stellar generations ([Jofré et al. 2017](#)). Hence, each chemical abundance measured from a stellar spectrum can be understood as a trait for reconstructing the chemical evolution of the Galaxy.

Of course, not all chemical elements are informative traits for chemical evolution studies, because in reality some of them may change through stellar lifetime. There are inner processes in stellar evolution such diffusion ([Dotter et al. 2017](#)) or planet formation/engulfment ([Meléndez et al. 2009](#); [Tucci Maia et al. 2019](#)) that alter the chemical composition in stars. Other inner mixing processes produced during dredge-up or induced thanks

to rotation can alter abundances such as $[C/N]$ or Li ([Masseron et al. 2017](#); [Aguilera-Gómez et al. 2018](#)). Nowadays we have to assume that a selection of chemical abundances remain approximately intact in FGK main-sequence stars and can be used to trace chemical evolution.

Few years ago, [da Silva et al. \(2012\)](#) studied several traits for chemical evolution studies of solar-type stars. In particular, $[Y/Mg]$, $[Sr/Mg]$, $[Y/Zn]$ and $[Sr/Zn]$ showed a significant trend as a function of age for their entire sample. When performing a linear fit of $[Y/Mg]$ as a function of stellar age for a sample of nearby solar twins, [Nissen \(2015\)](#) obtained slope of ~ 0.04 dex/Gyr and interpreted this relation using nucleosynthesis arguments, namely that massive stars produced Mg and expelled it into the interstellar medium at a different timescale than intermediate-mass reaching the AGB and producing Y. This has motivated discussions about the possibility of using abundance ratios as “chemical clocks”, in particular if ages are difficult to measure. The exact dependency of $[Y/Mg]$ or $[Ba/Mg]$ with age is still debated as it seems to further depend on stellar properties such as metallicity ([Feltzing et al. 2017](#); [Skúladóttir et al. 2019](#)) but not evolutionary state, at least before the AGB phase ([Slumstrup et al. 2017](#)). In addition to $[Y/Mg]$ and $[Ba/Mg]$, $[Al/Y]$ also have shown similar dependencies with ages ([Nissen 2016](#); [Spina et al. 2016](#)), at least for solar twins.

Several other works that benefit from accurate age estimates have studied trends of abundance ratios as a function of age ([Bedell et al. 2018](#); [Spina et al. 2018](#); [Delgado Mena et al. 2019](#); [Feuillet et al. 2018](#), to mention recent works). Most of these analyses have been restricted to using abundance ratios in their classical form, namely as a function of iron. Motivated by the fact

that the “chemical clocks” discussed above do not include iron, we searched for other combinations in a sample of 30 elemental abundances. We found 55 relations that are as significant as those previously mentioned. This new set of ratios can be used for the same applications as $[Y/Mg]$. In addition, they can be applied to models of Galaxy evolution and used to build stellar phylogenies (Jofré et al. 2017, Jackson et al. in prep). In this letter we report these findings.

2. Data and Methods

We considered the sample of 80 solar twins (including the Sun) analysed by Bedell et al. (2018, and references therein) and Spina et al. (2018). This is the largest sample of Solar Twins analysed using the differential technique for high-precision estimates of the abundances of 30 elements as well as stellar ages. The ages and abundance data, as well as the list of stars, can be found in these papers referenced.

In short, Bedell et al. (2018) and Spina et al. (2018) measured chemical abundances using HARPS@La Silla spectra taken from the public ESO Science Archive Facility. The spectra have very high resolving power (100,000). For multiple observations, the spectra were stacked to achieve very high signal-to-noise of above 200 pix^{-1} . In addition, spectra taken with the MIKE@Las Campanas of slightly lower resolution (65,000 to 80,000) but equal SNR were used to complement the wavelength ranges not covered by HARPS. This allowed the researchers to measure abundances of elements like oxygen from the O triplet at 770 nm. Stellar parameters and abundances were derived using 1D LTE analysis based on equivalent widths. Stellar ages were estimated using fits to isochrones following the same procedure as described in Spina et al. (2018).

We considered all possible combinations of abundance ratios of all 30 elements and performed a linear regression fit to these ratios as a function of age. Unlike Bedell et al. (2018) and Spina et al. (2018), we considered all stars, including the very old ones that are suspected to be part of the thick disk and could follow a different chemical enrichment history. The regression fit was done using the python 2.7 routine `stats.linregress` from the `scipy` library.

Only the traits whose linear fit had an absolute slope greater than 0.03 dex/Gyr and a correlation factor greater than 0.7 were considered. Choosing that threshold for the slope is motivated by the normally lower than 0.03 dex/Gyr slope seen in the linear fits of abundance ratios as a function of Fe by Bedell et al. (2018). We were interested in finding relations that are as significant as the $[Y/Mg]$ or $[Ba/Mg]$ relations discussed in the literature, which have a slope greater than 0.03 dex/Gyr. We note that different fitting techniques, selection of stars, thresholds for the slopes and correlation coefficients might yield slightly different results and therefore a different final sample of selected traits. Therefore, the results of the linear fits of all abundance combinations as a function of age can be found in the online material.

3. Results

The linear correlation coefficients for the selected traits are listed in Table 1. The fit is further plotted in Figure 1 alongside with the abundance ratio for each star as a function of age. Each trait is plotted in a different panel, and is indicated in the top left side.

For better interpretation of the results, at the bottom right side of each panel we have added two boxes with labels and colours, which help to attribute the chemical element involved

in the trait to a nucleosynthesis family. The left-hand side box represents the family of the element in the numerator while the right-hand side box represents the family of the element in the denominator of the abundance ratio. The families were chosen following the classification indicated in Table 2. This classification comes from discussions in Nomoto et al. (2013), except the neutron-capture family, for which we simply considered the elements analysed by Spina et al. (2018). As extensively discussed in that work (see also Bisterzo et al. 2014; Karakas & Lugaro 2016; Battistini & Bensby 2016), it is difficult to disentangle how much of these elements is produced by the slow neutron-capture process (s) and how much by the rapid neutron-capture process (r), each having a different site. This is why we decided to include all elements in the same family here.

We note that Nomoto et al. (2013) did not consider titanium as an α -capture element, since this element’s theoretical prediction does not match the observations (Kobayashi et al. 2006). However, observationally Ti behaves like an α -element, at least in terms of the abundance trends as a function of $[Fe/H]$, which is why we include it in this family. Carbon belongs to a special family that we call *sa*, because carbon has multiple unique formation sites. It can be produced in AGB stars, via s -process, or from massive stars, via α -capture (see Amarsi et al. 2019, for extensive discussions). While other elements are also produced by a variety of channels, carbon’s mass production is believed to be significant in all these channels.

We find that all selected traits involve different families. The ratios selected here consider elements in their $[X/Fe]$ form with opposite (increasing vs. decreasing) trends with age. In fact, Spina et al. (2018) obtained negative trends of the n -capture elements in their $[X/Fe]$ form as a function of age, and Bedell et al. (2018) obtained both positive and negative slopes for the other elements. The traits found here correspond to abundance ratios of elements that showed a general positive trend in their $[X/Fe]$ vs. age correlation in Bedell et al. (2018).

We further find that the denominator of our selected abundance ratios is always a n -capture element, including the already studied traits $[Mg/Y]$ and $[Mg/Ba]$. The slopes in our fits are 0.042 and 0.047 dex/Gyr, respectively. This agrees well with previous findings (Nissen 2015; Tucci Maia et al. 2016). The n -capture elements selected here are known to have more than 50% contribution from the s -process in the Sun (see Spina et al. 2018, for a discussion on this sample). The percentages were calculated by Bisterzo et al. (2014). Elements with lower percentage in s -process contribution for the solar abundances (like Eu, Sm, or Dy) were not selected to vary enough with age, according the restrictions imposed in this analysis. The trend of $[C/Ba]$ with age has the largest slope in our sample of 0.049 ± 0.003 dex/Gyr. This puts a constraint on the maximum change of abundance ratio with age for this sample of solar metallicity stars.

The final 55 abundance ratios contain 6 with carbon, 17 with α -capture elements, 10 with iron-peak elements and 22 with odd- Z elements. Among the α -capture, we obtain traits including O, Mg, Si and Ti. The element S was not selected. Among the iron-peak, we obtain traits including Mn, Co, Ni and Zn. It is interesting that Fe was not selected, since it is the standard element used for abundance ratios. Cr was also not selected. Regarding the odd- Z , we find Na, Al, Sc and Cu selected, but not V.

In order to investigate the abundance ratios further, we grouped the traits by the different n -capture elements or by the families of the numerator of the abundance ratios. The mean and standard deviation of the slopes for each of the groups can be

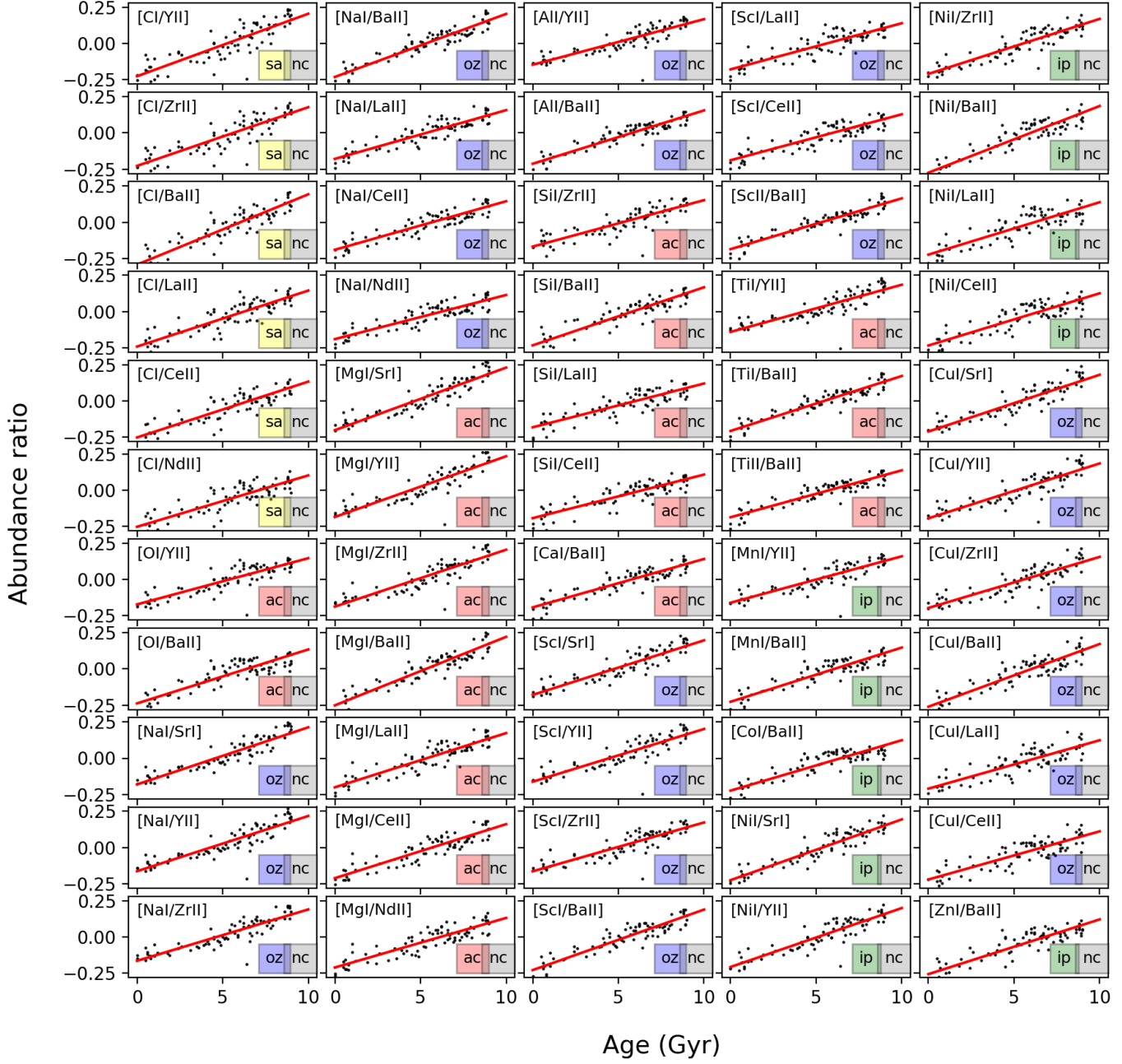


Fig. 1: Selected abundance ratios as a function of age in solar twins together with the linear fits of the trends. The abundance ratio is indicated in each panel at the top left, while at the bottom right the nucleosynthetic family of each abundance in a different colour (see Table 2 for the definition of each label).

found in Table 3, where we also indicate the total number a given abundance/family was selected.

Regarding the n -capture elements, the largest mean slopes are obtained for Sr and Ba, although the mean slope for Ba has the largest standard deviation. However, there is no relation between the the solar s -process percentage contribution and the

slopes for the age trends, if we consider the values adopted by Spina et al. (2018) which are obtained by Bisterzo et al. (2014).

When looking at the mean slopes of the different families, carbon is the one with the largest mean slope, but they all seem to be of comparable magnitudes, especially when considering their standard deviations. These results can be further visualised

Table 1: Linear regression fit coefficients. Error: standard error ($\times 10^2$); r^2 : correlation coefficient

Trait	slope (dex/Gyr)	intercept dex	error (dex/Gyr)	r^2	Trait	slope (dex/Gyr)	intercept dex	error (dex/Gyr)	r^2
[CI/YII]	0.043	-0.226	0.304	0.721	[CI/BaII]	0.049	-0.293	0.255	0.822
[CI/ZrII]	0.040	-0.228	0.277	0.733	[CI/CeII]	0.038	-0.252	0.234	0.777
[CI/LaII]	0.039	-0.242	0.245	0.762	[OI/YII]	0.032	-0.171	0.229	0.713
[CI/NdII]	0.035	-0.252	0.248	0.724	[NaI/SrI]	0.039	-0.181	0.267	0.736
[OI/BaII]	0.037	-0.238	0.240	0.754	[NaI/ZrII]	0.035	-0.165	0.212	0.783
[NaI/YII]	0.038	-0.164	0.239	0.765	[NaI/LaII]	0.034	-0.180	0.195	0.792
[NaI/BaII]	0.043	-0.231	0.187	0.874	[NaI/NdII]	0.030	-0.190	0.185	0.775
[NaI/CeII]	0.033	-0.190	0.177	0.820	[MgI/YII]	0.042	-0.185	0.255	0.776
[MgI/SrI]	0.043	-0.202	0.281	0.752	[MgI/BaII]	0.047	-0.252	0.201	0.876
[MgI/ZrII]	0.039	-0.187	0.232	0.786	[MgI/CeII]	0.037	-0.211	0.204	0.810
[MgI/LaII]	0.037	-0.201	0.221	0.786	[AlI/YII]	0.031	-0.146	0.219	0.725
[MgI/NdII]	0.034	-0.212	0.212	0.769	[SiI/ZrII]	0.032	-0.168	0.235	0.703
[AlI/BaII]	0.037	-0.213	0.172	0.854	[SiI/LaII]	0.030	-0.182	0.211	0.724
[SiI/BaII]	0.040	-0.233	0.219	0.811	[CaI/BaII]	0.033	-0.192	0.179	0.817
[SiI/CeII]	0.030	-0.193	0.205	0.734	[ScI/YII]	0.036	-0.162	0.246	0.737
[ScI/SrI]	0.038	-0.180	0.274	0.707	[ScI/BaII]	0.042	-0.229	0.204	0.843
[ScI/ZrII]	0.034	-0.164	0.223	0.745	[ScI/CeII]	0.032	-0.189	0.200	0.763
[ScI/LaII]	0.032	-0.178	0.221	0.727	[TiI/YII]	0.033	-0.141	0.238	0.705
[ScII/BaII]	0.035	-0.186	0.153	0.870	[TiII/BaII]	0.032	-0.187	0.163	0.834
[TiI/BaII]	0.038	-0.207	0.169	0.865	[MnI/BaII]	0.037	-0.227	0.204	0.812
[MnI/YII]	0.032	-0.160	0.226	0.720	[NiI/SrI]	0.042	-0.225	0.253	0.779
[CoI/BaII]	0.035	-0.224	0.208	0.781	[NiI/ZrII]	0.038	-0.210	0.221	0.791
[NiI/YII]	0.041	-0.208	0.226	0.805	[NiI/LaII]	0.036	-0.224	0.251	0.727
[NiI/BaII]	0.046	-0.275	0.234	0.832	[CuI/SrI]	0.039	-0.211	0.270	0.729
[NiI/CeII]	0.036	-0.234	0.238	0.745	[CuI/ZrII]	0.035	-0.196	0.236	0.741
[CuI/YII]	0.038	-0.194	0.243	0.757	[CuI/LaII]	0.033	-0.210	0.240	0.712
[CuI/BaII]	0.043	-0.261	0.223	0.828	[ZnI/BaII]	0.038	-0.257	0.231	0.773
[CuI/CeII]	0.033	-0.221	0.234	0.720					

Table 2: Nucleosynthetic families of elements considered in this study. The label is used as reference in Figure 1.

family	label	elements
Carbon	sa	C
α -capture	ac	O, Mg, Si, S, Ca, Ti
odd-Z	oz	Na, Al, Cu, Sc, V
iron-peak	ip	Cr, Mn, Fe, Co, Ni, Zn
n -capture	nc	Sr, Y, Zr, Ba, La, Ce Pr, Nd, Sm, Eu, Gd, Dy

in Figure 2, where we plot the mean slope and standard deviation of the mean for each family. The first panel contains all selected n -capture elements, while the second and third panels show the results for Ba and Y, because these were shown to contribute to ratios of elements in all families. We note that for Ba and Y, the error bar of the sa family corresponds to the uncertainty of the linear fit (see Table 1 for [C/Ba] and [C/Y], respectively). All family combinations behave similarly, with C systematically yielding higher slopes.

4. Discussion

Neutron-capture elements, in particular those produced by the s -process, have shown to add crucial information in chemical evolution studies (see recent study of Skúladóttir et al. 2019). Their gradual and slow production as intermediate-mass stars reach the AGB phase and produce stellar winds carrying the

Table 3: Mean slopes and their standard deviation for traits separated by n -capture element or by family. The number column indicates the times this particular element/family was selected

Element family	number	mean slope dex/Gyr	std. dev dex/Gyr
Ba	16	0.039	0.005
Ce	7	0.034	0.003
La	7	0.034	0.003
Nd	3	0.033	0.002
Sr	5	0.040	0.002
Y	10	0.037	0.004
Zr	7	0.036	0.003
ac	17	0.036	0.005
ip	10	0.038	0.004
oz	22	0.036	0.004
sa	6	0.041	0.004

newly synthesised elements into the ISM. Hence, new generations of stars formed within this environment will inherit a gradual increase of s -process elements. Since the production of s -process depends on the overall metallicity of the progenitor star (Karakas & Lugaro 2016), the enrichment of s -process elements is very dependent on the local conditions and star formation history of the previous generations.

With this in mind, the relation of [Mg/Y] or [Mg/Ba] as a function of age has been explained with chemical evolution principle in the literature. It is thus expected that not only would these

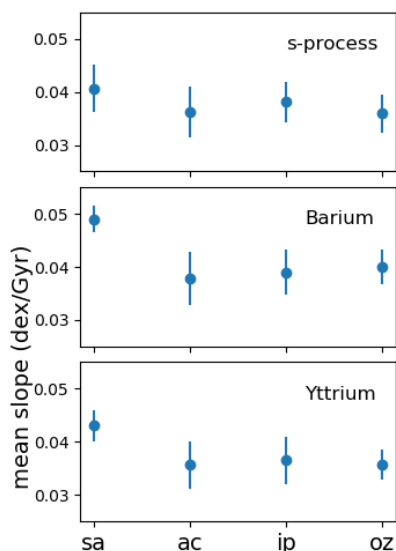


Fig. 2: Mean and standard deviations of slopes grouped by their families. The first panel corresponds to all selected n -capture elements while the second and third panel consider only the results for Ba and Y, respectively.

2 ratios show significant trends as a function of stellar age, but other ratios involving both α -capture and s -process elements, such as the other 15 cases resulting from our exercise, would as well. Although C behaves as both α -capture and n -capture element, the fact we find 6 traits with strong dependency of C over a s -process element with age suggests that the C contribution to chemical evolution from s -process is lower than from α -capture, at least at solar metallicities. This reasoning might contradict the results of Amarsi et al. (2019) who studied the [C/O] ratio for different stellar populations. The fact that this ratio is negative for halo stars and zero for disk stars, suggests that the carbon's s -process contribution plays an important role as metallicity increases. That conflicts with our reasoning that slopes in trends of abundance ratios with age increase if production sites for the elements differ. Our sample however contains stars of same metallicity but different ages. Limongi & Chieffi (2018) presented an extensive study of nucleosynthesis of massive stars obtaining that the relative production of C with respect to O increases with metallicity. The large slopes of C with respect to several s -process elements found here offer new alternatives to study the production mechanisms of this element.

The relation of the odd- Z element Al with respect to Y has also caught the attention in the literature (Nissen 2016). It is explained following similar nucleosynthetic arguments as for [Mg/Y], that the rapid production of Al in core-collapse SNe of massive stars is compensated with the increasing contribution of Y from lower-mass AGB stars in time. Na is produced in a similar way as Al, being alternatives to stellar population studies (Hawkins et al. 2015). In Nissen (2016) it is further discussed how [Cu/Na] remains constant over time, suggesting a similar production site for these elements. Our traits for the odd- Z family contain both Cu and Na elements with respect to similar n -capture elements.

Ni seems to be the iron-peak element with the strongest influence, which could be explained by the strong [Na/Ni] correlation found for these type of stars (Nissen 2015) and the strong positive [Ni/Fe] correlation found by Bedell et al. (2018). It is

interesting to note that while we set the threshold for selecting our traits above the typical slopes found for [X/Fe], we do select iron-peak elements. This means that iron-peak family does not necessarily have a weaker dependency with age when considering its ratio with s -process abundances (see Table 3). The iron-peak family has indeed a variety of mechanisms to create elements, and is expelled to the interstellar medium by different supernovae. [Mn/Fe], for example, has significant trends as a function of [Fe/H], and Zn is also greatly produced by very massive stars (Kobayashi et al. 2006).

5. Conclusion

We present the results of abundance ratios as a function of stellar ages for a set of 80 solar twins for which 30 different chemical elements were measured with high precision by Bedell et al. (2018, and references therein). By selecting only the trends whose linear fit yielded a correlation factor above 70% and a slope above 0.03 dex/Gyr we found 55 abundance ratios, including the widely discussed [Mg/Y] and [Mg/Ba] “chemical clocks”.

All of them included two different nucleosynthetic families, and all included one n -capture element whose s -process percentage to the solar abundance is larger than the r -process one. The maximum slope found was for [C/Ba] of $\sim 0.05 \pm 0.003$ dex/Gyr. There seems to be no abundance ratio evolving faster than ~ 0.05 dex/Gyr in solar twins.

The new era of industrial stellar abundances from on-going and future spectroscopic surveys has just begun, and is already providing the community with datasets of chemical abundances of elements in all families considered here (Jofré et al. 2019). In particular, thanks to Gaia and seismic missions such as *Kepler* or *TESS*, it is becoming possible to estimate age distributions of many stars in the Milky Way. Investigating how the traits for chemical evolution found here behave in different conditions can provide new insights for constraining the chemodynamical models of the formation and evolution of our Galaxy. Much of this information is already available, we should take the opportunity to explore it by considering abundance ratios as a function the s -process elements.

Acknowledgements. We thank the referee for their positive and thoughtful comments, which helped to significantly order the discussions. We warmly acknowledge K. Yaxley, D. Boubert and P. Das for lively discussions on evolution of traits in general. We further acknowledge support from the MIT International Science and Technology Initiatives (MISTI) grant, which funded H.J. research visit from which these results were obtained. P.J. is partially funded by FONDECYT Iniciación grant Number 11170174. M.T. and P.J. thank the Joint Committee ESO-Chile for postdoctoral financial support, and ECOS-Conicyt for enabling travel and relevant discussions that lead to this paper.

References

- Aguilera-Gómez, C., Ramírez, I., & Chanamé, J. 2018, *A&A*, 614, A55
- Amarsi, A. M., Nissen, P. E., & Skúladóttir, Á. 2019, *A&A*, 630, A104
- Battistini, C., & Bensby, T. 2016, *A&A*, 586, A49
- Bedell, M., Bean, J. L., Meléndez, J., et al. 2018, *ApJ*, 865, 68
- Bisterzo, S., Travaglio, C., Gallino, R., Wiescher, M., & Käppeler, F. 2014, *ApJ*, 787, 10
- da Silva, R., Porto de Mello, G. F., Milone, A. C., et al. 2012, *A&A*, 542, A84
- Delgado Mena, E., Moya, A., Adibekyan, V., et al. 2019, *A&A*, 624, A78
- Dotter, A., Conroy, C., Cargile, P., & Asplund, M. 2017, *ApJ*, 840, 99
- Feltzing, S., Howes, L. M., McMillan, P. J., & Stokutė, E. 2017, *MNRAS*, 465, L109
- Feuillet, D. K., Bovy, J., Holtzman, J., et al. 2018, *MNRAS*, 477, 2326
- Freeman, K., & Bland-Hawthorn, J. 2002, *ARA&A*, 40, 487
- Hawkins, K., Jofré, P., Masseron, T., & Gilmore, G. 2015, *MNRAS*, 453, 758
- Jofré, P., Das, P., Bertranpetit, J., & Foley, R. 2017, *MNRAS*, 467, 1140

- Jofré, P., Heiter, U., & Soubiran, C. 2019, *ARA&A*, 57, 571
- Karakas, A. I., & Lugaro, M. 2016, *ApJ*, 825, 26
- Kobayashi, C., Umeda, H., Nomoto, K., Tominaga, N., & Ohkubo, T. 2006, *ApJ*, 653, 1145
- Limongi, M., & Chieffi, A. 2018, *ApJS*, 237, 13
- Masseron, T., Lagarde, N., Miglio, A., Elsworth, Y., & Gilmore, G. 2017, *MNRAS*, 464, 3021
- Meléndez, J., Asplund, M., Gustafsson, B., & Yong, D. 2009, *ApJ*, 704, L66
- Nissen, P. E. 2015, *A&A*, 579, A52
- . 2016, *A&A*, 593, A65
- Nomoto, K., Kobayashi, C., & Tominaga, N. 2013, *ARA&A*, 51, 457
- Skúladóttir, Á., Hansen, C. J., Salvadori, S., & Choplin, A. 2019, *arXiv e-prints*, arXiv:1908.10729
- Slumstrup, D., Grundahl, F., Brogaard, K., et al. 2017, *A&A*, 604, L8
- Spina, L., Meléndez, J., Karakas, A. I., et al. 2016, *A&A*, 593, A125
- . 2018, *MNRAS*, 474, 2580
- Tucci Maia, M., Meléndez, J., Lorenzo-Oliveira, D., Spina, L., & Jofré, P. 2019, *A&A*, 628, A126
- Tucci Maia, M., Ramírez, I., Meléndez, J., et al. 2016, *A&A*, 590, A32